MJFAS MALAYSIAN JOURNAL OF FUNDAMENTAL AND APPLIED SCIENCES
PRINT ISSN: 2289-5981 | ONLINE ISSN: 2289-599X

RESEARCH ARTICLE

Heated laterite as a low-cost adsorbent for arsenic removal from aqueous solution

Syaiful Akhmal Saadon [a], Salmiati [b,*], Abdull Rahim Mohd Yusoff [c,d], Zulkifli Yusop [b], Shamila Azman [a], Davin Uy [e], Achmad Syafiuddin [a]

[a] *Department of Environmental Engineering, Faculty of Civil Engineering, Universiti Teknologi Malaysia, 81310 Skudai, Johor, Malaysia*
[b] *Centre for Environmental Sustainability and Water Security (IPASA), Research Institute for Sustainable Environment, Universiti Teknologi Malaysia, 81310 Skudai, Johor, Malaysia*
[c] *Department of Chemistry, Faculty of Science, Universiti Teknologi Malaysia, 81310 Skudai, Johor, Malaysia*
[d] *Ibnu Sina Institute for Scientific and Industrial Research (ISI-SIR), Universiti Teknologi Malaysia, 81310 Skudai, Johor, Malaysia*
[e] *Institute of Research and Training, No. 14, St 185, Chamkarmorn, Phnom Penh, Cambodia*

* *Corresponding author: salmiati@utm.my*

Article history
Submitted 10 July 2017
Revised 2 October 2017
Accepted 2 January 2017
Published Online 8 Mac 2018

Graphical abstract

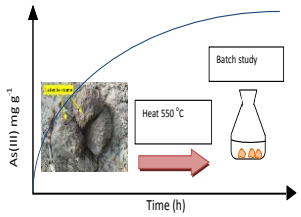

Abstract

Existing works reported that the laterite prepared using chemical treatment improved its removal performance compared to the raw laterite. However, this treatment has several drawbacks such as costly and potentially produces pollutant. To overcome this issue, the present work proposed heated laterite (HL) for removal of Arsenic (III) (As(III)) from aqueous solution as a low-cost adsorbent without any chemical use. HL was firstly obtained via the heat treatment a temperature of 550 °C for raw material with geometric sizes of 0.6 to 1.0 mm. Properties of HL in terms of surface morphology, energy dispersive X-ray, porosity, surface area, and Fourier transform infrared spectroscopy were then characterized. Effects of physicochemical parameters such as pH, agitation speed, adsorbent dosage, and initial concentration for optimal adsorption performance of As(III) were investigated. Gibbs free energy, enthalpy, and entropy of the adsorption were also determined, from which the sorption capacity and isotherm were estimated using Langmuir and Freundlich isotherm models. Langmuir model was found to be more reliable than Freundlich in describing the process behavior. This study found that the removal performance of HL was strongly affected by the physicochemical parameters. As the main finding, the optimal conditions for a low-cost and green adsorbent were adsorbent dose of 6 g L^{-1}, with an initial As(III) concentration of 0.5 mg L^{-1}, pH 7, and agitation speed of 250 rpm, which successfully removed 98.8% of As(III).

***Keywords*:** Laterite, arsenic removal, heat treatment, adsorption isotherms

INTRODUCTION

Arsenic is a well-known human carcinogen [1,2]. It commonly exists in the natural water sources in two oxidation states namely arsenite (As(III)) and arsenate (As(V)), depending on the pH of the surrounding environment and its redox conditions. Its stable form , As(V), which dominates in the surface water, while As(III) exists in the groundwater [3]. The toxicity of arsenic relies greatly on its forms, for instance, As(III) is 60 times more toxic than As(V) [4]. Lethal diseases such as hyper-keratosis, hyper-pigmentation, conjunctivitis, disorders of the central nervous system, and peripheral vascular system were caused by long-term consumption of arsenic contaminated water at very low concentration of 0.01 to 0.05 mg L^{-1}[5]. Concerning these negative impacts to the human health, most countries implemented the maximum permissible limit of arsenic in drinking water to be 10 µg L^{-1} as recommended by the World Health Organization (WHO) [6].

The presence of arsenic in water environment has been well-established. For instance, arsenic in groundwater has been observed in various countries such as Bangladesh (12 ppb – 587 ppb) [7-9], India (6 ppb – 1219 ppb) [9,10], China (1 ppb – 950 ppb) [11], Vietnam (12 ppb – 884 ppb) [12], and Cambodia (1 ppb – 1150 ppb) [13]. The aforementioned discussions revealed that the concentration of arsenic was above the allowable limit regulated by WHO.

To date, there exist several methods employed to remove As(III) from contaminated water sources including oxidation, precipitation, coagulation, filtration, adsorption, ion exchange, and filtration processes [14]. Among these, adsorption is the most popular method because of its high removal efficiency, low cost, and environment-friendly [15]. Therefore, the above-mentioned facts showed that the adsorption seemed to be a good strategy to be implemented to remove the arsenic contaminant from the water.In general, the efficiency of the adsorption greatly depends on the nature of adsorbent, maximum loading capacity, selectivity, and affinity towards the target adsorbate [16]. Specifically for As(III) removal, different kinds of natural and synthetic materials such as bagasse fly ash-iron coated and sponge iron char [17], magnetic nanoparticles impregnated chitosan beads [6], leonardite [18], polyaniline/polystyrene nanocomposite [19], cobalt ferrite nanoparticles aggregated schwertmannite [20], polyvinyl pyrrolidone K25 coated cassava peel carbon [21], modified microporous activated carbon [22], laterite [23], and sulfidogenic fixed-bed column bioreactor [24] were well implemented. The current technologies also find the removal of As(III) using mesoporous Fe/Al bimetallic particles [25], an oxalic acid complex [26], and zirconia (ZrO_2) embedded in carbon nanowires [27].

Laterite has recently received a greatly attention for arsenic removal because of its removal performance and abundant availability in the world [28] and [29]. Laterite is a natural rock that commonly

contains iron, aluminum, silica, and titanium oxides. Intensive works were carried out to investigate its removal performance using acid treatment [15], $FeCl_3$ treatment [28], acid-base treatment [30], impregnating it with the α-MnO_2 nanorods [31], and polyacrylonitrile laterite mixed matrix ultrafiltration membrane [32] compared to its raw form. Recently, As(III) can be greatly removed using the acid-base treated laterite under the optimal condition at pH 5, 20 g L^{-1} adsorbent dose, and 300 min contact time [29]. The above-mentioned studies have significantly contributed to the removal of arsenic by laterite using the chemical treatment. However, this procedure has several drawbacks such as expensive and potentially produce new toxin or pollutant. Therefore, an alternative approach that is low-cost and without usage is needed.

Aligning to the aforementioned research gap, the present work aims to propose the use of heated laterite for removal of Arsenic (III) from aqueous solution as a low-cost and chemical-free adsorbent. This procedure has the potential to be an environmental friendly procedure for the removal purpose.

EXPERIMENTAL

Materials

As(III) solution was prepared by dissolving $NaAsO_2$ (Fluka, Steinheim, Germany) into the ultrapure water to get the 1000 ppm stock solution. The ultrapure water was obtained from Milli-Q water purification system (Massachusetts, USA). The pH of the adsorbate solutions was adjusted with 0.1 M HC (acid) or 0.1 M NaOH (base). All the glass apparatus used were cleaned by soaking in HNO_3 overnight followed by washing with the deionized water and then dried in an oven at a temperature of 50 ˚C.

Preparation of adsorbent

The laterites were collected from Kg. Tom province, Cambodia. They were then crushed by a jaw crusher and washed thrice with the tap water to remove loosely bound particles such as decomposed organic matter, sand, and dust. After dried in the natural environment, the laterites were sieved to get particles in geometric sizes of 1.0 to 0.6 mm. They were then stored in capped bottles after burned for 1 hour in Muffle Furnace (Carbolite, UK) at a temperature of 550 ºC. In this procedure, the adsorbent was prepared from free chemical usage.

Characterization of adsorbent

Field Emission Scanning Electron Microscopy-Energy Dispersive X-ray (FESEM-EDX, Supra 35VP, Merlin and Sigma, Germany) at an acceleration voltage of 15 kV and a working distance of 9.3 mm was used for adsorbent imaging morphology and elemental analysis (after the adsorbent particles were coated with gold). Porosity and surface area of the adsorbent were measured using Brunauer–Emmett–Teller (BET) surface analyzer (B-Flex, Micromeritics, USA) at bath temperature of 77.315 ºK, warm free space of 21.5688 cm^3, cold free space of 69.2643 cm^3, and equilibration interval of 1.0 g cm^{-3}. Fourier Transform Infrared (FTIR) spectra were recorded with FTIR spectrometer (Perkin Elmer Instrument, Frontier, Spectrum One, Germany) in the wavelength range of 450 - 4000 cm^{-1} using the KBr pellet technique.

Batch experiment for As(III) removal

The determination of As(III) removal by heated laterite (HL) was conducted by firstly transferring a 100 mL aliquot of the As(III) solution into a 250-mL Erlenmeyer flask. A 5 g L^{-1} of adsorbent was added to the flask containing the As(III) solution. The flask was placed in the incubator shaker (Protech, S1-100D, Malaysia) at a rotation speed of 150 rpm and a temperature of 25 ºC. The pH effect was investigated by adjusting As(III) solution from pH 3 to pH 11. The temperature effect on the adsorption of As(III) was studied over the range from 20 to 30 ºC. To determine the optimum adsorbent dose, the experiments were carried out using various adsorbent doses from 1 to 7 g L^{-1}. The agitation speed effect was evaluated for the range of 50 to 250 rpm. To determine the effect of adsorbate initial concentration, different concentration of As(III) solutions, 250, 500, 750, 1000, 1250, and 1500 ppb, were reacted with 6 g L^{-1} of adsorbent. All batch experiments were repeated three times. The varied batch parameters are listed in Table 1.

Table 1 List of batch parameters.

Varied parameter	pH	Temp. (Cº)	Agitation (rpm)	Adsorbent dosage (g L^{-1})	Initial conc. (ppb)
pH	3 - 11	25	150	5	500
Temperature	7	20 - 30	150	5	500
Agitation	7	30	50 - 250	5	500
Adsorbent dosage	7	30	250	1 - 7	500
Initial concentration	7	30	250	6	250 - 1250

The isotherm study was conducted by performing the adsorption of As(III) into both raw laterite (RL) and HL in batch experiments. The experimental details before the optimum batch condition can be described as follows: initial [As] 500 - 1250 ppb; pH 7; adsorbent dosage 5 g L^{-1}; temperature 25 Cº; contact time 10 h; agitation 150 rpm. Details for HL after the optimum batch condition are: initial [As] 500 - 1750 ppb; pH 7; adsorbent dosage 6 g L^{-1}; temperature 30 Cº; contact time 10 h; agitation 250 rpm. The As(III) concentration was then determined using inductively couple plasma mass spectrometry (ICP-MS, ELAN 6100, Perkin Elmer, USA), which has the following conditions; RF power 1350 W, gas flow plasma 13 L min^{-1}, auxiliary flow 0.95 L min^{-1}, integration time 0.2 s, sampling period 0.31 s, dead time 35 s, sample depth 7.0 mm. All treated samples were diluted to reach a maximum of 60 ppb of total arsenic and were acidified to 1% of (v/v) HNO_3.

Thermodynamics, kinetics and isotherm modeling

For the thermodynamics investigation, the Gibbs free energy (ΔG^0), enthalpy (ΔH^0) and entropy (ΔS^0) of adsorption were calculated using the following equations:

$$K_0 = \frac{C_{ad}}{C_e} \quad (1)$$

$$\Delta G = -RTlnK_o \quad (2)$$

$$lnK_0 = \frac{\Delta S^\circ}{R} - \frac{\Delta H^\circ}{RT} \quad (3)$$

where C_{ad} is the reduction of adsorbate concentration of the solution at equilibrium due to adsorption (mg L^{-1}), C_e the equilibrium concentration of the arsenic in the solution (mg L^{-1}), R is the universal gas constant (8.314 J mol K^{-1}), T is the temperature (K), and K_o is the equilibrium constant.

The kinetic data were then analyzed by the pseudo-first and pseudo-second orders models expressed below:

$$q_t = q_e[1 - \exp(-k_1 t)] \quad (4)$$

$$q_t = \frac{k_{s2} q_e^2 t}{1 + k_{s2} q_e t} \quad (5)$$

where q_e is the amount of As(III) sorption at equilibrium (mg g^{-1}), q_t is the amount of As(III) sorption at specific time (mg g^{-1}), t is the time (min), and k_1 and k_2 are the rate constants (min^{-1}). k_2 can be determined from k_{s2} and q_e values using the following relationship [33,34]

$$k_2 = k_{s2} q_e \quad (6)$$

The kinetic parameters were estimated by performing a non-linear analysis using the above-mentioned equations.

The adsorption capacity was estimated using the following mass equilibrium equation:

$$q = \frac{(C_0 - C_e)V}{m} \quad (7)$$

with c_0 and c_e are the initial and equilibrium concentrations, respectively. V is the experimental volume expressed in liters and m is the adsorbent mass expressed in grams. In order to estimate the sorption capacity and isotherm, Langmuir and Freundlich isotherm models were fitted to the data.

Langmuir [35] proposed a theoretical equilibrium isotherm relating the amount of gas absorbed on a surface to the pressure of the gas. It is a widely applied that demonstrates good agreement with a wide variety of experimental data. It can be expressed as follows:

$$q_e = \frac{q_m k_a c_e}{1+k_a c_e} \quad (8)$$

where c_e is the equilibrium concentration (mg L^{-1}), q_e the amount of As(III) adsorbed (mg g^{-1}), q_m is the q_e for a complete monolayer (mg g^{-1}), and k_a is a sorption equilibrium constant (L mg^{-1}).

The empirical model by Freundlich [36] is the earliest known sorption isotherm equation. It can be applied to non-ideal sorption on heterogeneous surface or multilayer sorption, which can be expressed as follows:

$$q_e = k_F c_e^{1/n_e} \quad (9)$$

where k_F and n are the isotherm constants, respectively.

RESULTS AND DISCUSSION

Characterization of adsorbent

Fig. 1 demonstrates the FESEM images of both RL and HL. It is apparent that RL has low porosity with heterogeneous surface texture. For HL, the creation of fractures on the surface can be observed. This is attributed to the rejection/release of carbon dioxide and water molecules from inside of laterite, resulted from the organic compounds decomposition via dehydroxylation reaction.

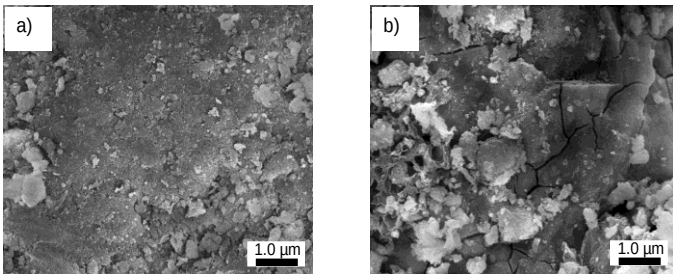

Fig. 1 FESEM images of (a) raw laterite and (b) heated laterite.

Surface area, total area, and volume in pores of RL and HL are listed in Table 2. It is clear that aforementioned values of HL were slightly increased compared to RL.

Table 2 Brunauer–Emmett–Teller analysis for raw and heated laterites.

Parameters	RL	HL
Surface area (m^2 g^{-1})	103.638	110.373
Total area in pores (m^2 g^{-1})	23.852	25.027
Total volume in pores (cm^3 g^{-1})	0.083	0.089

The EDAX results confirm that Al, Si, Fe and Ti of HL increase compared to RL (see Table 3). Conversely, the percentages of carbon and oxygen were considerably decreased in HL compared to RL. The increased percentage of metal elements in HL can be associated with the loss of total weight of adsorbent caused by the decomposition of organic. These findings are in line with the result obtained by [37], which observed that Fe increases in laterite after acid treatment.

Table 3 EDAX data analysis for laterite before and after adsorption of As(III).

Element	Weight %	
	RL	HL
Carbon	11.59	3.52
Oxygen	45.71	34.94
Aluminum	1.25	2.16
Silicon	2.45	2.47
Manganese	1.15	0
Iron	37.33	49.11
Ti	0.31	0.41

The X-ray diffraction (XRD) of raw and heated laterite is depicted in Fig. 2. It can be observed that the raw laterite (RL) has several diffraction peaks at 2θ = 21.24º, 26.58º, 33.40º, 36.80º, 40.24º, 41.30º, 53.48º, 59.10º, 61.58º and 68.28º (PCPDF card no. 010746399). The peaks represented intensified goethite (α-FeOOH). After heat treatment at a temperature of 550 ºC, the intensified hematite (α-Fe_2O_3) was observed in the heated laterite (HL) with diffraction peaks at 2θ = 20.00º, 24.18º, 26.62º, 33.18º, 35.70º, 40.86º, 49.56º, 54.12º, 62.54º and 64.08º (PCPDF card no. 010738433). Gialanella et al. [38] reported that the heat treatment changed the mineralogical phase of laterite from goethite to hematite. During the heat treatment, the directions of (100), (010) and (001) in goethite were transferred to (001), (110) and (111) directions in the trigonal hematite cell. In addition, Ruan et al. [39] confirmed that the structure of hematite consisted of layers of iron ions and layers of oxygen ions perpendicular to the triad axis.

Composition and microstructure influenced the kinetics of the dehydration of goethite with a water release equal to 10.1 wt%. The release of OH^- groups and decomposition of organic compounds in raw laterite (goethite) increased the existence of spherical pores and fractures on the surface of heated laterite (hematite). This was supported and verified by the characterization of FESEM and BET. The crystal structure of hematite was developed from 250 to 300 ºC. However, in this study, the temperature of heat treatment was increased up to 550 ºC in order to decompose the organic compounds present in the raw laterite.

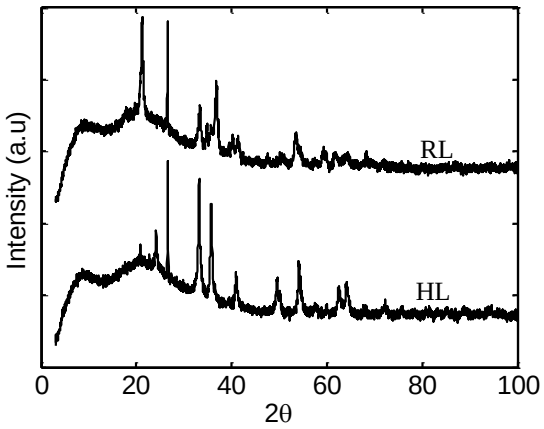

Fig. 2 X-ray diffraction pattern of raw laterite (RL) and heated laterite (HL).

FTIR spectra of RL and HL are depicted in Fig. 3. It can be observed that there is a broad stretch at 3370-3405 cm^{-1} and sharp peaks at 3625 and 3715 cm^{-1} confirming the presence of hydroxyl group (bonded-OH stretch). The band at 1620-1640 cm^{-1} assigns to interlayer water molecules between the adsorbent layer, 912 cm^{-1} with Al-OH bond stretching, and 543 and 474 cm^{-1} with Fe-O bond stretching. The sharp bands appeared at 1025 cm^{-1} and 1005 $cm^{-1}$is due to Si-O-Fe and Si-O vibrations, respectively. The bands in the region of 1526 – 1812 cm^{-1} are responsible to the mica group (phyllosilicate minerals). All observed peaks for HL are more

intensified than RL. The intensified peaks are attributed to the presence of higher amount of major groups in HL compared to RL.

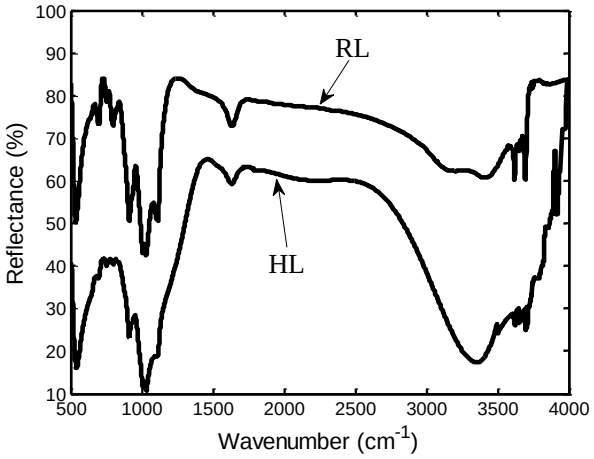

Fig. 3 FTIR spectrum of raw laterite (RL) and heated laterite (HL).

Effects of physico-chemical parameters

pH

In order to observe the effect of pH on the adsorption of As(III), the percentage of As(III) removal was assessed at different ranges of pH solutions in the batch experiment. Fig. 4(a) illustrates that the percentages of As(III) removal by HL are 89 - 94% for pH 3 to 9. However, the removal was drastically decreased at pH 10 and above. The species of ions in an aqueous solution is mainly determined by the pH and the dissociation constants. As(III) is stable as neutral H_3AsO_3 at pH below 9.1 and dominant as an anionic $H_2AsO_3^-$ at pH range between 9.1 and 12.1 [6]. Consequently, it can be identified that the neutral As(III) species has been adsorbed by HL via weak van der Waals forces of attraction [40]. Moreover, the pH point of zero charge (pH_{PZC}) is an important factor, and pH_{PZC} of laterite is 7.5. It is well-known that a solid surface is positively charged when the pH is below pH_{PZC}, and vise versa.

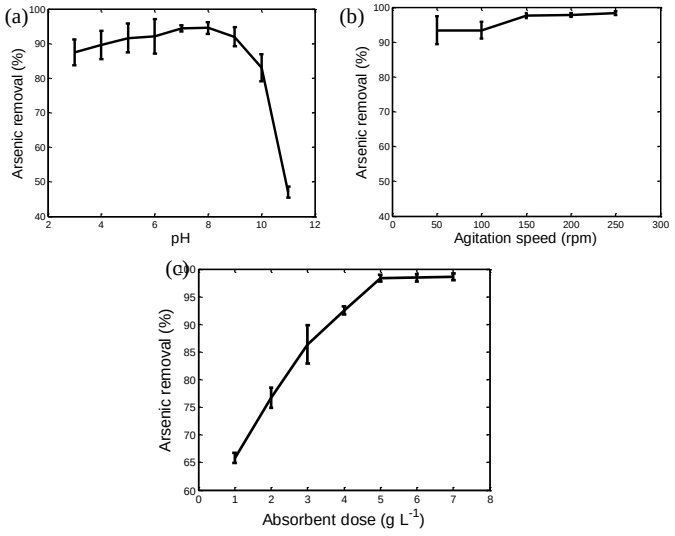

Fig. 4 Effect of a) pH, b) agitation speed, and c) adsorbent dosage on the percentage (%) of As(III) removal.

The adsorption of As(III) is divided into two processes, surface complexation (pH < 9.1) and electrostatic interactions (pH > 9.1). The adsorption of As(III) by hydrous iron and/or aluminum oxide by HL surface is mainly by ligand exchange [41]. The ligand exchange is envisaged as follows:

$$MOH_{(s)} + H_3AsO_{3(aq)} \rightarrow MH_2AsO_3 + H_2O \quad (10)$$

with M as iron or aluminum. The percentage of removal is found to be rapidly decreased with increasing pH. At higher pH (>9.1), As(III) adsorption is reduced due to the existence of a repulsive force between negatively charged HL and $H_2AsO_3^-$ anions, as As(III) is dominant as anion species ($H_2AsO_3^-$) in that pH range.

The adsorption mechanism at higher pH may be expressed by binding the negative species to the partially positive surface. Similarly, Maji et al. [42] found that the As(III) adsorption by activated alumina and iron-oxide coated sand is pH-independent. Also, iron and aluminum oxide present in the laterite played critical role in the As(III) adsorption. In this study, maximum As(III) adsorption on HL was observed at pH 7 ($\leq pH_{PZC}$ of HL). Based on this result and considering the environmental conditions in the ground water, subsequent experiments in this study were carried out at pH 7.

Agitation

For adsorption in the batch reactor, agitation quality is an important parameter for mass transfer process [43]. In addition, it is also essential for adsorption phenomena because of its effect on the outer boundary layer. The effect of agitation speed (50, 100, 150, 200 and 250 rpm) on As(III) adsorption was examined with 5 g L^{-1} of adsorbent, 500 ppb initial concentration of As(III) at 30 °C and pH 7. Fig. 4(b) shows that As(III) adsorption strongly depends on the speed of agitation as adsorption gradually increases with agitation up to 250 rpm.

As shown in Fig. 4(b), significant amount of As(III) was removed at 50 rpm (0.093 mg g^{-1}). The uptake of As(III) was improved (0.0984 mg g^{-1}) when the agitation speed was increased to 250. This can be interpreted as the reduction of convective resistance due to agitation. In general, when the agitation speed increased from 50 to 250 rpm, the percentage of As(III) removal increased from 93.3% to 98.3% (Fig. 4(b)). Therefore, the subsequent experiments were conducted at 250 rpm.

It was reported from the previous work that the mass transfer increased with the increase in agitation, resulting in an increase in the solute transport from the bulk solution to the adsorbent active site and thereby increasing the percentage of removal[41]. These results are in line with those of other studies and suggested that the rise of the agitation speed caused the decrease in the mass transfer resistance between the absorbate and adsorbent [44]. Alternatively, it was also found that the percentage of arsenic removal was increased when the agitation speed increased from 25 to 150 rpm[45]. However, they also found that the percentage of arsenic removal was decreased when the agitation speed increased higher than 150 rpm. This is due to the random collisions between particles and limits the contact time between arsenic ions to make bond with adsorbent surface.

Adsorbent dosage

The effects of adsorbent dosage on the percentage of removal As(III) is presented in Fig. 4(c). The maximum (98.88%) adsorption of As(III) was achieved at the adsorbent dose between 5 and 7 g L^{-1}. The increase in the percentage removal of As(III) can be attributed to the increase of the adsorbent surface area, pores, and active sites available for mass transfer, thus, more As(III) was adsorbed in the presence of higher laterite dosage. A further increment of the adsorbent dose did not influence much the adsorption due to non-availability of adsorbate. This result is consistent with those of other research which found that when the adsorbent dosage increased over the optimum dosage, the percentage of removal was slowly increased to a maximum value. The adsorbent dosage that is higher than the optimum value had a lower impact on As(III) sorption percentage [46]. It is due to unsaturation of some binding site and strong limitation on As(III) mobility [47]. In addition, it may be due to the two stages of arsenic adsorption i.e. fast formation of mono layer followed by slow plateau stage [48].

Effect of initial concentration

In order to evaluate the sorption mechanism and equilibration time for the maximum uptake, the sorption of As(III) on HL was studied as a function of contact time with different initial concentrations of As(III) (0.25, 0.5, 0.75, 1.0, and 1.25 mg L^{-1}) and the results are

shown in Fig. 5. Obviously, As(III) adsorption on HL was increased from 0.04 mg g^{-1} to 0.19 mg g^{-1} when the initial As(III) concentration increased from 0.25 mg L^{-1} to 1.25 mg L^{-1}. It confirmes that As(III) adsorption was increased with initial concentration of As(III). Further, this behavior can be associated with the increase in the driving force of the concentration gradient to overcome all mass transfer resistances, as an increase in the initial As(III) concentration. Such phenomenon is common in a batch reactor with both constant adsorbent dose and varying initial adsorbate concentration or vice versa [49].

However, the results show that the percentage of As(III) adsorption was gradually decreased from 97.5 to 89.3% when increasing the initial concentration from 0.25 mg L^{-1} to 1.25 mg L^{-1}. This may be related to the exhaustion of the sorption sites available on the adsorbent, for a given adsorbent dosage, when the As(III) concentration was increased [50]. Rapid As(III) adsorption was noted at the initial 60 min, due to the occurrence of sorbate and sorbent interactions with the negligible interference of solute-solute interaction [51]. The decrease of As(III) adsorption with increasing contact time is due to the decrease in the accessible sorption sites and the Columbic inhibition between the solute species readily sorbed and the solute species available at the interface for sorption [33].

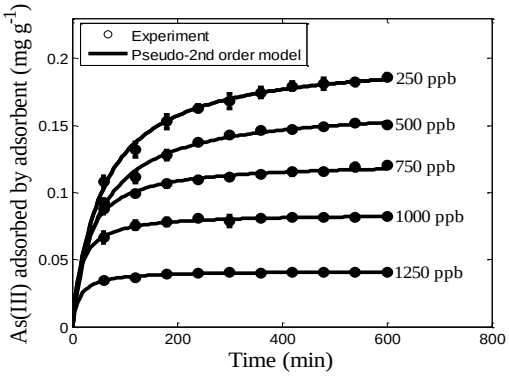

Fig. 5 Effect of initial concentration on As(III) adsorption.

Adsorption isotherms

The experimental results were then fitted to both Langmuir and Freundlich isotherms and the obtained parameters are listed in Table 4. Langmuir model is found to be more reliable than Freundlich, since better values of correlation coefficients are exhibited thus suggesting monolayer sorption and existence of constant sorption energy during the experimental conditions [52].

Table 4 Langmuir and Freundlich constants for As(III) adsorption by heated laterite.

Model	Parameter	RL	HL	HL(Optimum)
Langmuir	q_m (mg g^{-1})	0.10	0.16	0.21
	b (L mg^{-1})	48.1	49.3	46.6
	$b.q_m$(L g^{-1})	4.97	7.89	10.16
	R^2	0.99	0.99	0.94
Freundlich	K_f	0.11	0.19	0.30
	1/n	0.17	0.23	0.28
	R^2	0.90	0.90	0.93

The isotherm parameters in Table 4 were determined using the nonlinear regression analysis and the corresponding isotherm plots are shown in Fig. 6. The results show that the isotherm plateau has been reached due to the limiting value of the solid phase concentration. Considering both two and three parameters of HL, the Freundlich isotherm is found to have no physical significance in the adsorption process. The experimental data obtained in the present study when applied on the two-parameter isotherm models follows the order: Langmuir > Freundlich isotherms, similar to the previous report by Linsha et al. [53]. The high values of R^2 infer that the three-parameter models best fit the adsorption equilibrium data. The maximum adsorption capacity q_e obtained from Langmuir model for HL is 0.21 mg g^{-1}. Therefore, the best fitting isotherm model for HL is determined to be Langmuir rather than Freundlich.

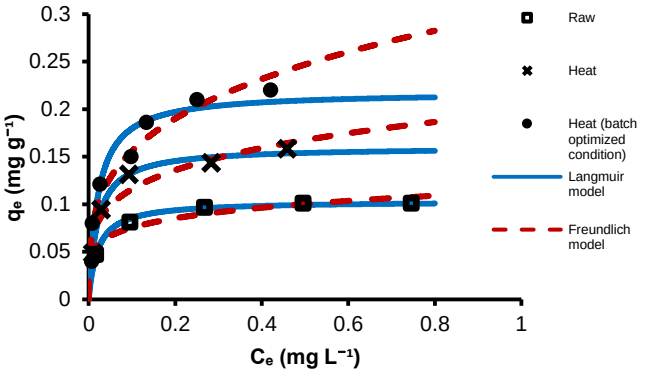

Fig. 6 Langmuir and Freundlich isotherms for the adsorption of As(III) onto raw laterite (RL), heating laterite (HL) before optimum batch condition and heating laterite (HL) after optimum batch condition.

The heating technique has led to an increase in q_e of laterite from 0.10 to 0.16 mg g^{-1}. Furthermore, the optimization of the batch condition also increased the adsorption capacity of heated laterite from 0.16 to 0.21 mg g^{-1}. Optimization of batch condition is done by increasing the temperature, adsorbent loading, and agitation speed during the adsorption experiment. Langmuir model produces two constants, which are q_m(mg g^{-1}) = maximum capacity and b (L mg^{-1}) = adsorption energy. The multiplication of q_m with b produces the value of tendency of adsorbate head towards the adsorbent surface. The higher the value of $q_m b$, the greater the tendency of the adsorbate towards the adsorbent surface. A comparison of $q_m b$ among various types of adsorbent can be referred in Maiti et al. [37]. Furthermore, Table 4 shows the increase of $q_m b$ after the heating and optimization of the batch condition.

Kinetic modeling

The R^2 values obtained in the current study indicated that the kinetics of As(III) sorption reaction with HL described by the pseudo-second order model is more reliable than the pseudo-first order model under the presented conditions reaction (Table 5). This is due to the fact that the pseudo-first order kinetic model cannot fit well the whole time range. However, this is usually applicable only at the initial stage of the adsorption process. All kinetically controlled reactions showed a better fit relationship to the pseudo-second order model since the calculated q_e is closer to that of the experimental where the R^2 is found to be 0.99. The pseudo-second order model is based on the assumption that the rate-determining step may be a chemical sorption involving valence forces through the sharing of electrons between adsorbent and adsorbate. Therefore, the pseudo-second order kinetic model is considered feasible to describe the adsorption process of As(III) on HL.

Table 5 Adsorption kinetic parameters for As(III) adsorption process.

C_0 (mg L^{-1})	Pseudo-first order			Pseudo-second order		
	k_1 (min^{-1})	q_e (mg g^{-1})	R^2	k_2 (min^{-1})	q_e (mg g^{-1})	R^2
0.25	1.66	0.04	0.97	0.07	0.04	0.99
0.5	1.68	0.08	0.96	0.07	0.09	0.99
0.75	1.20	0.11	0.92	0.04	0.12	0.99
1.0	1.0	0.14	0.83	0.02	0.17	0.99
1.25	0.89	0.16	0.81	0.02	0.20	0.99

The pseudo-second order kinetic model fitted at different initial concentrations of As(III) are presented in Fig. 5. The predicted q_e are found to have good agreement with the experimental equilibrium adsorption capacity. For example, predicted q_e by the pseudo-second order model for initial As(III) concentrations of 0.25, 0.5, 0.75, 1.0 and 1.25 mg L^{-1} are 0.04, 0.09, 0.12, 0.17 and 0.2 mg g^{-1} compared to experimental data as 0.04, 0.08, 0.12, 0.15 and 0.18 mg g^{-1}, respectively. The values of both k_1 and k_2 are found to be increasing with decreasing initial As(III) concentration [6]. At lower As(III) concentration, the adsorption rate is higher due to more availability of active sites on the adsorbent particle with less competition. However, at a higher initial As(III) concentration, all As(III) species are not able to come in contact with active sites of adsorbent (adsorption is much more competitive) and the rate of adsorption is slower, resulting in the lower rate constant values. For example, the value of k_2 decreases to 0.02 from 0.06 min^{-1} when initial As(III) concentrations are taken to be 1.25 instead of 0.25 mg L^{-1}. Ho [54] stated that the adsorption mechanism is mainly chemisorptions, when it follows the pseudo-second order kinetic model. So, As(III) adsorption on HL is chemisorptions in nature.

Thermodynamics modeling

In order to check the effects of temperature on adsorption process, the adsorption experiment was performed with different temperatures from 20 to 30 °C. The experimental observation indicates that the percentage of As(III) adsorption onto HL is increased from 89.5 to 97.6% at 30 °C (Fig. 7). Therefore, further adsorption experiments were carried out at 30 °C.

The results of the qualitative estimation of ΔH^0 and ΔS^0 can be obtained from the slope and intercept of the Van't Hoff plot, $\ln K_0$ vs. 1/T, as shown in Fig. 7(b)and listed in Table 6. Change in the Gibbs free energy is defined as the driving force for a system to reach a chemical equilibrium. The negative value of Gibbs free energy (ΔG^0) means that the adsorption was a spontaneous and favorable reaction. The ΔG^0 values decreased with an increase in temperature, indicating that a higher temperature could promote the removal efficiency of As(III). The decreasing value of ΔG^0 with increasing temperature suggests that the spontaneity degree of the adsorption process increases at a higher temperature [55,56].

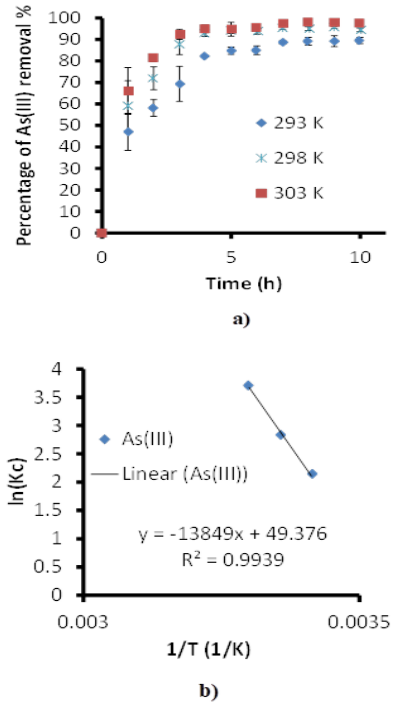

Fig. 7 Effect of batch temperature on As(III) adsorption.

ΔG^0, found to be below 8 kJ mol^{-1}, is consistent with a physical adsorption involving electrostatic interaction between adsorption sites and the adsorbate ion. Moreover, it has been noted that if the value of ΔG^0 is between 8 and 16 kJ mol^{-1}, the adsorption proceeds via a chemical ion exchange contribution. The more negative ΔG^0 values imply chemisorptions mechanism by forming stable complexes on the adsorbent surface [57]. Positive values of ΔH^0 (128.32 kJ mol^{-1}) indicates the endothermic nature of the overall adsorption process of As(III) onto HL. The endothermic adsorptions can be correlated to a stronger interaction between As(III) and HL surface [58].

The higher value of ΔH^0 means that the adsorption process might be due to the physico-chemical adsorption process rather than a purely physical or chemical adsorption process as heats of chemisorptions generally fall into a range of 80 to 200 kJ mol^{-1}. Positive values of ΔS^0 (0.46 kJ K^{-1} mol^{-1}) implies that the adsorbent and adsorbate have high affinity so that the adsorption process could easily occur. In addition, the positive value of ΔS^0 reflects the increased randomness at the solid-solution interface during adsorption, and it also indicates the occurrence of ion replacement reactions. The low value of ΔS^0 reveals no remarkable change in entropy during the adsorption process.

Table 6 Thermodynamic parameters for As(III) adsorption process.

Initial As(III) concentration (mg L^{-1})	ΔH^0 (kJ mol^{-1})	ΔS^0 (kJ K^{-1} mol^{-1})	ΔG^0 (kJ mol^{-1})		
			293K	298K	303K
0.5	128.32	0.46	-5.22	-7.01	-9.33

CONCLUSION

This paper evaluated the performance of heated laterite (HL) as a low-cost adsorbent for removal of Arsenic (III) from aqueous solution. For currently considered case, the optimum parameters for removal efficiency of HL are at a temperature of 30 °C and pH 7. About 98.8% of As(III) was removed using the proposed adsorbent with a dose of 6 g L^{-1} and an initial As(III) concentration of 0.5 mg L^{-1} under optimum conditions. It was observed that the rapid adsorption occured within the first hour of operation. The findings of this research therefore successfully characterized HL as the adsorbent for removal of Arsenic (III) without any chemical use. Further studies need to be carried out in order to validate its performance in the field.

ACKNOWLEDGEMENT

The present work was fully funded by Universiti Teknologi Malaysia and the Malaysian Ministry of Higher Education under CLMV grant -Vot. No. R.J30000.7809.4L187 (Effectiveness of arsenic and hygienic awareness module on the rural water supply in Cambodia).

REFERENCES

[1] T.R. Chowdhury, G.K. Basu, B.K. Mandal, B.K. Biswas, G. Samanta, U.K. Chowdhury, C.R. Chanda, D. Lodh, S.L. Roy, K.C. Saha, S. Roy, S. Kabir, Q. Quamruzzaman, D. Chakraborti, Arsenic poisoning in the Ganges delta, *Nature* 401 (1999) 545-546.

[2] M. Doucleffand N. Terry, Pumping out the arsenic, *Nat. Biotechnol.* 20 (2002) 1094-1095.

[3] A. Rahman, M.A. Rahman, A. Samad, A.M.S. Alam, Removal of arsenic with oyster shell : Experimental measurements, *Pak. J. Anal. Env. Chem.* 9 (2008) 69-77.

[4] R.N. Ratnaike, Acute and chronic arsenic toxicity, *Postgrad. Med. J.* 79 (2003) 391-396.

[5] P. Bhattacharya, A.H. Welch, K.G. Stollenwerk, M.J. McLaughlin, J. Bundschuh, G. Panaullah, Arsenic in the environment: Biology and chemistry, *Sci. Total Environ.* 379 (2007) 109-120.

[6] J. Wang, W. Xu, L. Chen, X. Huang, J. Liu, Preparation and evaluation of magnetic nanoparticles impregnated chitosan beads for arsenic removal from water, *Chem. Eng. J.* 251 (2014) 25-34.

[7] M. Sultana, T.J. Mou, S.K. Sanyal, F. Diba, Z.H. Mahmud, A.K. Parvez, M.A. Hossain, Investigation of arsenotrophic microbiome in arsenic-affected Bangladesh groundwater, *Groundwater* 55 (2017) 736-746.

[8] Z. Aziz, B.C. Bostick, Y. Zheng, M.R. Huq, M.M. Rahman, K.M. Ahmed, A. van Geen, Evidence of decoupling between arsenic and phosphate in shallow groundwater of Bangladesh and potential implications, *Appl. Geochem.* 77 (2017) 167-177.

[9] M.M. Rahman, Z. Dong, R. Naidu, Concentrations of arsenic and other elements in groundwater of Bangladesh and West Bengal, India: Potential cancer risk, *Chemosphere* 139 (2015) 54-64.

[10] T. Roychowdhury, H. Tokunaga, M. Ando, Survey of arsenic and other heavy metals in food composites and drinking water and estimation of dietary intake by the villagers from an arsenic-affected area of West Bengal, India, *Sci. Total Environ.* 308 (2003) 15-35.

[11] J. Zhang, T. Ma, L. Feng, Y. Yan, O.K. Abass, Z. Wang, H. Cai, Arsenic behavior in different biogeochemical zonations approximately along the groundwater flow path in Datong Basin, Northern China, *Sci. Total Environ.* 584 (2017) 458-468.

[12] L.H. Pham, H.T. Nguyen, C. Van Tran, H.M. Nguyen, T.H. Nguyen, M.B. Tu, Arsenic and other trace elements in groundwater and human urine in Ha Nam province, the Northern Vietnam: Contamination characteristics and risk assessment, *Environ. Geochem. Health* 39 (2017) 517-529.

[13] J. Buschmann, M. Berg, C. Stengel, L. Winkel, M.L. Sampson, P.T.K. Trang, P.H. Viet, Contamination of drinking water resources in the Mekong delta floodplains: Arsenic and other trace metals pose serious health risks to population, *Environ. Int.* 34 (2008) 756-764.

[14] Y.-h. Xu, T. Nakajima, A. Ohki, Adsorption and removal of arsenic (V) from drinking water by aluminum-loaded Shirasu-zeolite, *J. Hazard. Mater.* 92 (2002) 275-287.

[15] Y. Glocheux, M. Méndez, A.B. Albadarin, S.J. Allen, G.M. Walker, Removal of arsenic from groundwater by adsorption onto an acidified laterite by-product, *Chem. Eng. J.* 228 (2013) 565-574.

[16] P. Sathishkumar, M. Arulkumar, V. Ashokkumar, Modified phyto-waste Terminalia catappa fuit shells: a reusable adsorbent for the removal of micropollutant diclofenac, RSC Adv. 5 (2015) 30950-30962.

[17] L. Singh, B. Kumar, A. Kumar, K. Karar, Arsenic removal using bagasse fl y ash-iron coated and sponge iron char, *J. Env. Chem. Eng.* 2 (2014) 1467-1473.

[18] Y. Chammui, P. Sooksamiti, W. Naksata, S. Thiansem, Removal of arsenic from aqueous solution by adsorption on Leonardite, *Chem. Eng. J.* 240 (2014) 202-210.

[19] B. Davodiand M. Jahangiri, Determination of optimum conditions for removal of As (III) and As (V) by polyaniline/polystyrene nanocomposite, *Synt. Met.* 194 (2014) 97-101.

[20] A. Dey, R. Singh, M.K. Purkait, Cobalt ferrite nanoparticles aggregated schwertmannite : A novel adsorbent for the efficient removal of arsenic, *J. Wat. Proc. Eng.* 3 (2014) 1-9.

[21] R. Selvakumar, S. Kavitha, M. Sathishkumar, K. Swaminathan, Arsenic adsorption by polyvinyl pyrrolidone K25 coated cassava peel carbon from aqueous solution, *J. Hazard. Mater.* 153 (2008) 67-74.

[22] M. Asadullah, I. Jahan, M. Boshir, Preparation of microporous activated carbon and its modification for arsenic removal from water, *J. Ind. Eng. Chem.* 20 (2014) 887-896.

[23] A. Maiti, H. Sharma, J.K. Basu, S. De, Modeling of arsenic adsorption kinetics of synthetic and contaminated groundwater on natural laterite, *J. Hazard. Mater.* 172 (2009) 928-934.

[24] M. Altun, E. Sahinkaya, I. Durukan, S. Bektas, K. Komnitsas, Arsenic removal in a sulfidogenic fixed-bed column bioreactor., *J. Hazard. Mater.* 269 (2014) 31-7.

[25] Z. Cheng, F. Fu, D.D. Dionysiou, B. Tang, Adsorption, oxidation, and reduction behavior of arsenic in the removal of aqueous As(III) by mesoporous Fe/Al bimetallic particles, *Water. Res.* 96 (2016) 22-31.

[26] Q. Ge, G. Han, T.-S. Chung, Effective As(III) removal by a multi-charged hydroacid complex draw solute facilitated forward osmosis-membrane distillation (FO-MD) processes, *Environ. Sci. Technol.* 50 (2016) 2363-2370.

[27] J. Luo, X. Luo, C. Hu, J.C. Crittenden, J. Qu, Zirconia (ZrO_2) embedded in carbon nanowires via electrospinning for efficient arsenic removal from water combined with DFT studies, *ACS Appl. Mater. Interfaces* 8 (2016) 18912-18921.

[28] W.-y. Huang, R.-h. Zhu, F. He, D. Li, Y. Zhu, Y.-m. Zhang, Enhanced phosphate removal from aqueous solution by ferric-modified laterites: Equilibrium, kinetics and thermodynamic studies, *Chem. Eng. J.* 228 (2013) 679-687.

[29] V.K. Rathore, D.K. Dohare, P. Mondal, Competitive adsorption between arsenic and fluoride from binary mixture on chemically treated laterite, *J. Env. Chem. Eng.* 4 (2016) 2417-2430.

[30] A. Maiti, J.K. Basu, S. De, Chemical treated laterite as promising fluoride adsorbent for aqueous system and kinetic modeling, *Desalination* 265 (2011) 28-36.

[31] D.N. Thanh, M. Singh, P. Ulbrich, F. Štěpánek, N. Strnadová, As(V) removal from aqueous media using α-MnO_2 nanorods-impregnated laterite composite adsorbents, *Mater. Res. Bull.* 47 (2012) 42-50.

[32] S. Chatterjeeand S. De, Adsorptive removal of arsenic from groundwater using a novel high flux polyacrylonitrile (PAN)-laterite mixed matrix ultrafiltration membrane, *Environ. Sci.: Water Res. Technol.* 1 (2015) 227-243.

[33] K. Gupta, S. Bhattacharya, D. Nandi, A. Dhar, A. Maity, A. Mukhopadhyay, D.J. Chattopadhyay, Arsenic (III) sorption on nanostructured cerium incorporated manganese oxide (NCMO): A physical insight into the mechanistic pathway,*J. Colloid Interface Sci.* 377 (2012) 269-276.

[34] S. Hokkanen, E. Repo, S. Lou, M. Sillanpää, Removal of arsenic (V) by magnetic nanoparticle activated microfibrillated cellulose, *Chem. Eng. J.* 260 (2015) 886-894.

[35] I. Langmuir, The constitution and fundamental properties of solids and liquids. Part I. Solids, *J. Am. Chem. Soc.* 38 (1916) 2221-2295.

[36] H. Freundlich, Über die adsorption in lösungen, *Zeit. Phy. Chem.* 57 (1906) 385–470.

[37] A. Maiti, J.K. Basu, S. De, Experimental and kinetic modeling of As(V) and As(III) adsorption on treated laterite using synthetic and contaminated groundwater: Effects of phosphate, silicate and carbonate ions, *Chem. Eng. J.* 191 (2012) 1-12.

[38] S. Gialanella, F. Girardi, G. Ischia, I. Lonardelli, M. Mattarelli, M. Montagna, On the goethite to hematite phase transformation, *J. Thermal Anal. Cal.*102 (2010) 867-873.

[39] H.D. Ruan, R.L. Frost, J.T. Kloprogge, L. Duong, Infrared spectroscopy of goethite dehydroxylation: III. FT-IR microscopy of in situ study of the thermal transformation of goethite to hematite, *Spectrochim. Acta. A Mol. Biomol. Spectrosc.* 58 (2002) 967-981.

[40] D. Sánchez-Rivera, O. Perales-Pérez, F.R. Román, LC-ICPMS speciation of arsenite and arsenate oxyanion mixtures during their adsorption with dried sludge, *Anal. Methods* 5 (2013) 1583.

[41] A. Maiti, S. Dasgupta, J.K. Basu, S. De, Adsorption of arsenite using natural laterite as adsorbent, *Sep. Purif. Technol.* 55 (2007) 350-359.

[42] S.K. Maji, Y.-h. Kao, P.-y. Liao, Y.-j. Lin, C.-w. Liu, Implementation of the adsorbent iron-oxide-coated natural rock (IOCNR) on synthetic As(III) and on real arsenic-bearing sample with filter, *Appl. Surf. Sci.* 284 (2013) 40-48.

[43] B.A. Fil, M.T. Yilmaz, S. Bayar, M.T. Elkoca, Investigation of adsorbent of the dyestuff Astrazon Red Violet 3RN (Basic Violet 16) on montmonrillonite clay, *Brazilian J. Chem. Eng.* 31 (2014) 171-182.

[44] S. Mandal, S.S. Mahapatra, M.K. Sahu, R.K. Patel, Artificial neural network modelling of As(III) removal from water by novel hybrid material, *Process Saf. Environ. Prot.* 93 (2015) 249-264.

[45] U. Shafique, A. Ijaz, M. Salman, W.u. Zaman, N. Jamil, R. Rehman, A. Javaid, Removal of arsenic from water using pine leaves, *J. Taiwan Inst. Chem. Eng.* 43 (2012) 256-263.

[46] M. Aryal, M. Ziagova, M. Liakopoulou-Kyriakides, Study on arsenic biosorption using Fe(III)-treated biomass of *Staphylococcus xylosus*, *Chem. Eng. J.* 162 (2010) 178-185.

[47] P. Roy, N.K. Mondal, S. Bhattacharya, B. Das, K. Das, Removal of arsenic(III) and arsenic(V) on chemically modified low-cost adsorbent: batch and column operations, *Appl. Water. Sci.* 3 (2013) 293-309.

[48] P. Mondal, C.B. Majumder, B. Mohanty, Effects of adsorbent dose, its particle size and initial arsenic concentration on the removal of arsenic, iron and manganese from simulated ground water by Fe^{3+} impregnated activated carbon, *J. Hazard. Mater.* 150 (2008) 695-702.

[49] A. Bhatnagar, Y. Choi, Y. Yoon, Y. Shin, B.-h. Jeon, J.-w. Kang, Bromate removal from water by granular ferric hydroxide (GFH), *J. Hazard. Mater.* 170 (2009) 134-140.

[50] H. Muhamad, H. Doan, A. Lohi, Batch and continuous fixed-bed column biosorption of Cd^{2+} and Cu^{2+}, *Chem. Eng. J.* 158 (2010) 369-377.

[51] M. Alkan, M. Doğan, Y. Turhan, Ö. Demirbaş, P. Turan, Adsorption kinetics and mechanism of maxilon blue 5G dye on sepiolite from aqueous solutions, *Chem. Eng. J.* 139 (2008) 213-223.

[52] M. Aryaland M. Ziagova, Study on arsenic biosorption using Fe(III)-treated biomass of *Staphylococcus xylosus*, *Chem. Eng. J.* 162 (2010) 178-185.

[53] V. Linsha, P.S. Suchithra, A. Peer Mohamed, S. Ananthakumar, Amine-grafted alumino-siloxane hybrid porous granular media: A potential sol-gel sorbent for treating hazardous Cr(VI) in aqueous environment, *Chem. Eng. J.* 220 (2013) 244-253.

[54] Y.-S. Ho, Second-order kinetic model for the sorption of cadmium onto tree fern: A comparison of linear and non-linear methods, *Water Res.* 40 (2006) 119-125.

[55] P.D. Nemade, A.M. Kadam, H.S. Shankar, W. Bengal, Adsorption of arsenic from aqueous solution on naturally available red soil Pravin, *J. Environ. Biol.* 30 (2009) 499-504.
[56] M. Chiban, G. Carja, G. Lehutu, F. Sinan, Equilibrium and thermodynamic studies for the removal of As (V) ions from aqueous solution using dried plants as adsorbents, *Arab. J. Chem.* 9 (2012) S988-S999.
[57] Z. Özlem Kocabaş-Atakliand and Y. Yürüm, Synthesis and characterization of anatase nanoadsorbent and application in removal of lead, copper and arsenic from water, *Chem. Eng. J.* 225 (2013) 625-635.
[58] E. Haque, J.W. Jun, S.H. Jhung, Adsorptive removal of methyl orange and methylene blue from aqueous solution with a metal-organic framework material, iron terephthalate (MOF-235), *J. Hazard. Mater.* 185 (2011) 507-511.